Water Air Soil Pollut (2024) 235:713
https://doi.org/10.1007/s11270-024-07523-5

Effect of Halide Ions on the TiO_2-mediated Photocatalysis of Carbendazim in Aqueous Medium Under Near-ultraviolet Light Irradiation

Margherita Bragetta · Raimondo Germani · Matteo Tiecco · Husam B. R. Alabed · Tiziana Del Giacco

Received: 7 June 2024 / Accepted: 16 September 2024 / Published online: 30 September 2024

Abstract The degradation of carbendazim (CBZ) through TiO_2 photocatalysis, in the presence of halide ions and under near-UV light irradiation, was investigated. HPLC–MS technique was used to characterize the photoproducts. Spectrophotometric analysis showed that CBZ degraded slowly in TiO_2 aqueous dispersions containing no salt (CBZ conversion of 6% after ca. 5 h of irradiation). The photodegradation efficiency increased particularly by addition of bromide salts. Indeed, CBZ reached complete degradation after ca. 30 min at the maximum concentration of NaBr used (0.05 M). Two significant aspects have emerged from the data analysis: the bromide role is to cause inhibition of the electron–hole recombination, a reaction known to be competitive with the reactive process; CBZ photodegradation is especially initiated by direct hole transfer pathway, whereas the OH• role is crucial in the catalyst regeneration process. Degradation attempts under sunlight appeared promising for a more sustainable photocatalytic process.

Keywords Bromide · Carbendazim · Degradation · Electron transfer · Photocatalysis · Titanium dioxide

1 Introduction

Pesticides are widely applied to inhibit or kill phytopathogenic fungi in agriculture, which are the cause of crop losses (Khmelevtsova et al., 2024; Hu and Liu, 2024). Due to lack of proper wastewater discharge facilities, in recent years the increasingly widespread use of pesticides has affected the contamination of surface, groundwater and wastewater and this has been proven by the presence of these compounds in a wide range of environmental matrices (Kaur et al., 2024; Sousa et al., 2018). Many of the pesticides are toxic for the health, hazardous for environment and resistant to biodegradability, making them a significant concern for society and problematic for common treatment processes. Their adverse impact on human health and aquatic ecosystem is found all over the world (Ádám et al., 2024; Khan et al., 2020; Yadav and Devi, 2017). The industries associated with these types of pesticide production are facing challenges to accomplish removal of pesticides from wastewater.

Supplementary Information The online version contains supplementary material available at https://doi.org/10.1007/s11270-024-07523-5.

M. Bragetta · R. Germani · H. B. R. Alabed · T. Del Giacco (✉)
Department of Chemistry, Biology and Biotechnology, Centro Di Eccellenza Sui Materiali Innovativi Nanostrutturati (CEMIN), University of Perugia, Via Elce Di Sotto 8, 06123 Perugia, Italy
e-mail: tiziana.delgiacco@unipg.it

M. Tiecco
Chemistry Interdisciplinary Project (ChIP), School of Pharmacy, University of Camerino, Via Madonna Delle Carceri, 62032 Camerino, MC, Italy

Currently, most of the research activities in the field of wastewater treatment are involved in the development of innovative approaches with enhanced efficiency and large-scale applicability for pesticide removal (Saleh et al., 2020). Despite best efforts to regulate and engineer the use of pesticides, they continue to be detected and present problems at municipal water treatment plants worldwide (Tahmasebia et al., 2024). This points out a need for an alternative water treatment to various traditional methods (including physical adsorption, biodegradation and chemical precipitation) able of completely degrading pesticides, so as to preserve drinking water. Numerous investigations have been directed to the advanced oxidation processes (AOP) for the removal of organic pollutants as innovative methodology able to completely mineralize the targeted pollutants. AOPs therefore represent a chemical approach used to remove organic materials in wastewater via oxidation reactions by highly reactive hydroxyl radicals ($OH^{\bullet}$) produced in situ. AOPs can be classified as homogeneous systems (Fenton and photo-Fenton reactions) and heterogeneous systems (semiconductor photocatalytic process) (Cheng et al., 2016; Ghamarpoor et al., 2024; Shamim et al., 2024). Heterogeneous photocatalytic oxidation process employing TiO_2 as catalyst has demonstrated promising results for the degradation of persistent organic pollutants producing more biologically degradable and less toxic substances, showing great potential among developing green chemistry technologies. This semiconductor, however, shows some disadvantages that limit its application particularly on industrial scale, including low catalytic efficiency due to the quick recombination of the photogenerated electron–hole pairs and in utilizing solar light due to its large bandgap energy ($E_g = 3.2$ eV, accordingly $\lambda < 385$ nm) (Rengifo-Herrera and Pulgarin, 2023; Hadei et al., 2021; Kanan et al., 2020). Strategies to overcome these drawbacks of TiO_2 for applications in photocatalysis have concerned the doping and structural modification of the semiconductor particles (Jiang et al., 2021; Kaur et al., 2016; Rostami et al., 2022; Varma et al., 2020).

Since this topic is extremely crucial and of growing interest, our recently published works involved the oxidative degradation of polluting dyes catalyzed by TiO_2 in aqueous medium. These studies showed that the addition of cationic surfactants improved the pollutant photodegradation efficiency. This was attributed to the surfactant role to ensure greater proximity of the dye to the semiconductor surface, thus favoring the electron injection from the dye to the photogenerated positive hole (Anastasio et al., 2017; Del Giacco et al., 2017; Germani et al., 2021, 2023). Along this line, we have considered it worthwhile to extend these investigations to removal processes of pesticides from aqueous media by means of heterogeneous photocatalysis. In the present work, our attention was focused on carbendazim (CBZ, methyl (1*H*-1,3-benzimidazol-2-yl) carbamate), a substance widely used as fungicide to control diseases in cereal, vegetable and fruit plants. In a recent review, CBZ effects in the biological and environmental contamination were well underlined, particularly regarding ecological risks, toxicities and potential risks for human health (Zhou et al., 2023). CBZ could induce embryonic, reproductive, developmental and hematological toxicities of various animal models. This compound is long-time persistent and its degradation occurs slowly. Among the commonly used techniques to degrade CBZ, AOPs have become feasible and effective methods for wastewater treatment. These processes include the following chemical removal systems in aqueous medium: UV/H_2O_2 (Starling et al., 2019), Fenton (Da Costa et al., 2019), ozonation (Xiao et al., 2015) and UV/TiO_2 (Marcelino et al., 2019; Murgolo et al., 2021; Zhou et al., 2023). Direct photolysis, electrochemical oxidation and photoelectrocatalysis were tested too (Machado et al., 2022), although the mineralization of these pollutants is not always achieved, generating non-photodegradable by-products (Dos Santos et al., 2017). Even though several possible degradation pathways of CBZ were proposed, the degradation mechanism is not yet fully understood and remains elusive. The aim of our work is therefore not to degrade CBZ to mineralization, but rather to produce and identify the main degradation products and to formulate a possible mechanism. To have a better understanding of the CBZ transformation, we have investigated the photocatalyzed reaction by TiO_2 from a kinetic point of view, as for the pathways that lead to the major products. In particular, the role of additives, such as halide ions, on the reaction mechanism and photodegradation efficiency was discussed.

2 Materials and Methods

2.1 Materials

CBZ (Sigma-Aldrich), TiO_2 (P25, Degussa, dried at 110 °C) and sodium salts (NaBr, NaCl and NaI, Sigma-Aldrich) were analytical grade reagents. CTABr and TBABr were purchased from Sigma-Aldrich and recrystallized from acetone/methanol mixture before use (Baglioni et al., 2009). Distilled water (pH 5.5 − 6.0) was used for all photodegradation experiments. LC/MS-grade acetonitrile, water and formic acid used as mobile phase on liquid chromatography analysis were all acquired from Merck.

2.2 Photodegradation Experiments

For the photocatalytic tests, the suspended mixture, prepared by adding a weighed quantity of P25 TiO_2 powder (0.8 g/L) and ammonium or sodium salt to 50 mL of CBZ aqueous solution (5.0×10^{-5} M) at not controlled pH, was loaded into a reactor equipped with jacket filled with re-circulated water. This catalyst dose was found to be the amount that best optimized the photodegradation efficiency. The irradiated dispersion was kept at 30 °C by means of a thermostat under constant air-equilibrated and stirred condition. Explorative irradiations were carried out in an Applied Photophysics multilamp apparatus equipped with 12 phosphor-coated fluorescent lamps (15 W each) emitting around 355 nm ($\Delta\lambda_{1/2}=20$ nm), wavelengths absorbed above all by TiO_2. Before irradiation, the suspension was magnetically stirred in the dark for 30 min to reach equilibrated adsorption between TiO_2, CBZ and atmospheric oxygen. Some experiments were performed by irradiation with three LED OSRAM PARATHOM CLASSIC lamps (150 W each). The emission spectrum, shown in Supporting Information (Fig. S1), was recorded by a Avaspec-ULS2048CL-EVO spectrometer, equipped with AvaBench 75 mm optical fiber and 2048 pixel CMOS detector (grating 300 lines/mm). The experiments with CBZ under natural sunlight were performed following the procedure described above. Measurements were carried out on dispersions containing 1.0×10^{-2} M NaBr and exposed to sunlight in Perugia, Italy, in July (location 43°06′53″ N; 12°23′13″ E).

For product analysis, more concentrated dispersions in CBZ (2.0×10^{-4} M) and NaBr (4.0×10^{-2} M) were prepared, keeping unchanged the TiO_2 amount (0.8 g/L). This was necessary because of the lower sensitivity of the analytical technique used (see paragraph *2.3*). Photocatalysis experiments were carried out following the procedure above described.

2.3 Analytical Procedures

To evaluate the percentage of CBZ degradation, 2.0 mL of mixture samples were withdrawn from the reactor at variable time intervals. To recover quantitatively the pollutant adsorbed on TiO_2, 2.0 mL of ethanol were added into the sample. The catalyst was separated by filtration through a 0.2 µm-pore size membrane filter (Minisart RC, 15 mm diameter) after adequately shaking the suspension by vortex mixer. The filtrate was then transferred into a 4-ml quartz cuvette for UV/VIS analysis. Absorption spectra were recorded on an Agilent 8453 Diode Array UV–vis spectrophotometer. Observed rate constants for CBZ degradation at 30 °C were determined by monitoring the change of absorbance at an appropriate wavelength as a function of the irradiation time. The k values were the average of at least three determinations. The average error estimated on the observed rate constants was ± 10%.

The sampling for the product analysis was carried out following the above procedure, but ethanol was replaced with acetonitrile for the sample dilution. Agilent analyzer, which consists of Agilent 1260 Infinity II liquid chromatograph coupled with Agilent 6530 Accurate-Mass Q-TOF (Quadrupole-Time of Flight) analyzer and Agilent JetStream source, was used for HPLC–MS analyses. The chromatographic separation of analytes was carried out by a reverse phase C18 column (Ascentis Express Peptide ES-C18 with the dimensions of 75 × 2.1 mm and particle diameter 2.7 µm) maintained at 25 °C and 0.45 mL/min flow. The mobile phase consisted of a binary gradient of water (solvent A) and acetonitrile (solvent B). Both solvents were added with formic acid at a final concentration of 0.1%. The gradient was as follows: time 0 min B 2.5%; time 8 min B 60%, time 15 min: stop run. Injection volume was 0.23 µL. Spectrometric data (Full Scan mode) were collected in the 50–1700 m/z range in positive polarity. The Agilent JetStream source ran on the following protocol:

250 °C for the N_2 gas, 10 L/min for the drying gas, 35 psi for the nebulizer, and 300 °C at 12 L/min for the sheath gas. Spectrophotometric data (DAD) were collected in the 160–640 nm range.

The solid state absorption spectrum of TiO_2 was recorded by a portable instrument for combined reflectance, time-resolved and steady-state fluorescence based on the Time Correlated Single Photon Counting (TCSPC) technique was used.

3 Results and Discussion

3.1 Property of CBZ

The absorption spectrum of CBZ recorded in distilled water (pH 5.5–6), solvent used for all photodegradation experiments, is shown in Fig. 1. Three maxima in the UV region at 237 nm ($\varepsilon = 12{,}000$ L M^{-1}), 280 nm ($\varepsilon = 13{,}330$ L M^{-1}), 285 nm (14,730 L M^{-1}) and a shoulder at 293 nm were identified. The first band was assigned to the aliphatic chain linked to the imidazole group, while the two peaks at lower energy were attributed to $\pi \rightarrow \pi^*$ transition of the CBZ benzimidazole structure (Machado et al., 2022). A similar absorption spectrum was recorded at neutral pH by Boudina et al. (2003). Taking into account the pK_a values (4.5 and 10.6, Furini et al., 2016) CBZ was exclusively present in its neutral form at the pH used in the present study. As seen in Fig. 2, this form can be in equilibrium with the protonated and the deprotonated charged species ($CBZ(+H)^+$ and $CBZ(-H)^-$, respectively). The stability of both ionic forms is due to resonance of the positive and negative charge delocalized along the benzimidazole ring and the carbamate group (Fig. S2). This effect increases especially the basicity of the imidazolic nitrogen, although the highest charge density resides on the amidic nitrogen (Cheng and Li, 2022).

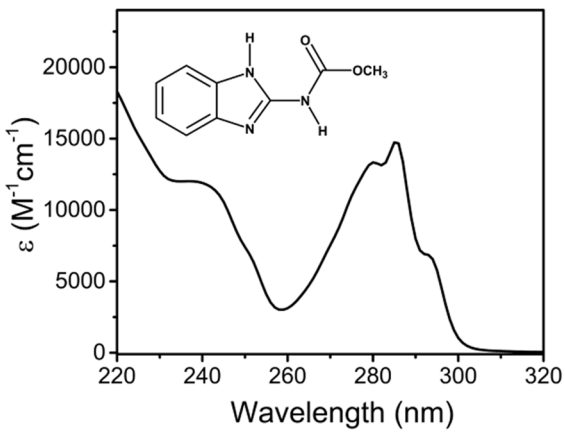

Fig. 1 Molecular structure of CBZ and its absorption spectrum recorded in neat water

3.2 TiO_2-photocatalyzed Degradation of CBZ Assisted by Bromide Salts

Preliminary experiments of CBZ (5.0×10^{-5} M) photodegradation were carried out on air-equilibrated aqueous dispersions of 0.8 g/L TiO_2 under UV radiation around 355 nm, wavelengths absorbed exclusively by the semiconductor, as inferred by the comparison of solid state TiO_2 spectrum with that of CBZ in aqueous solution (Fig. S3 and Fig. 1, respectively). As it can be seen, there was no significant CBZ degradation during the photolysis; only 6% of the initial concentration was degraded (estimated by the absorbance values at 286 nm) after 315 min of irradiation (Fig. 3). This proved some photocatalytic stability of the pesticide under our experimental condition.

Addition of 1.0×10^{-2} M NaBr produced instead considerable changes of the initial absorption spectrum of CBZ compared with those recorded at

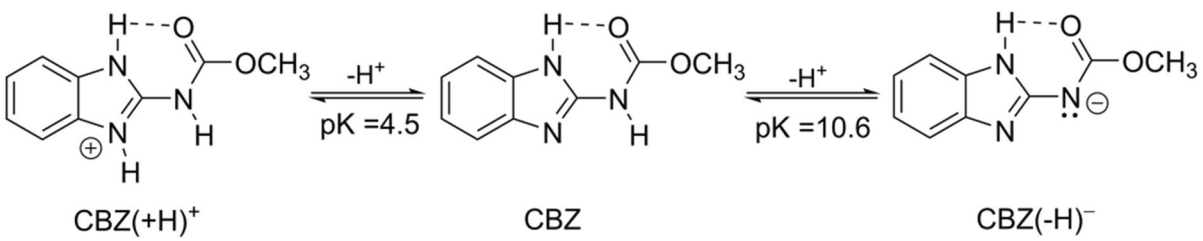

Fig. 2 Deprotonation equilibria in aqueous solution of CBZ

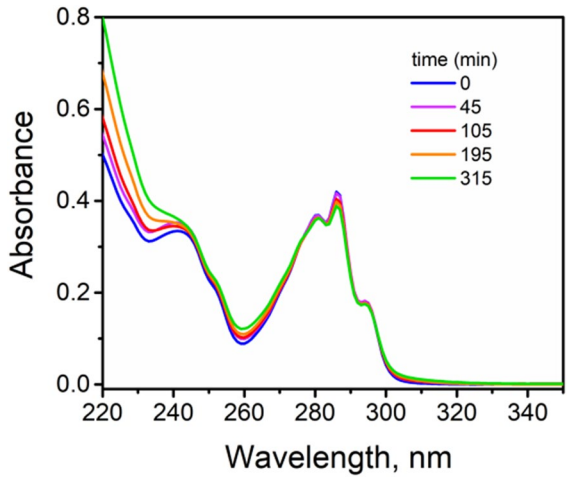

Fig. 3 Absorption spectra recorded during the irradiation of 0.8 g/L TiO_2 aqueous dispersion in the presence of 5.0×10^{-5} M CBZ (2.5×10^{-5} M after dilution with ethanol) as a function of irradiation time

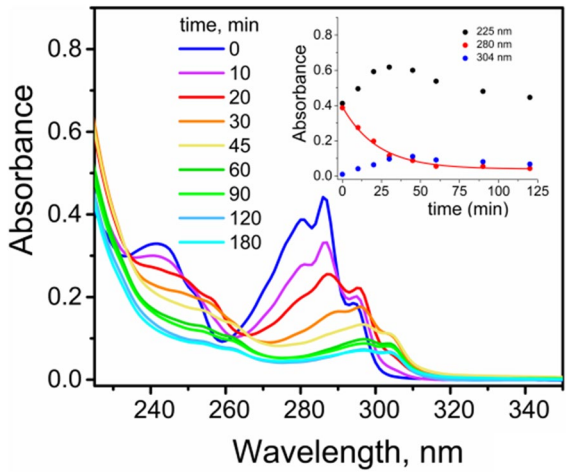

Fig. 4 Absorption spectra recorded during the photodegradation of 5.0×10^{-5} M CBZ (2.5×10^{-5} M after dilution with ethanol) catalyzed by 0.8 g/L TiO_2 in aqueous dispersion in the presence of 1.0×10^{-2} M NaBr as a function of irradiation time. Inset: changes in absorbance at 225, 280 and 304 nm as a function of irradiation time. The solid line represents the corresponding kinetic fitting

different irradiation times. In particular, as presented in Fig. 4, the initial CBZ bands were completely replaced within ca. 60 min by new absorptions below 235 nm and in the 300–320 nm region, wavelengths clearly absorbed by photodegradation products, the nature of which will be discussed later. By examining the kinetics, shown in the inset of Fig. 4, it can be observed that the decay of CBZ at $\lambda = 280$ nm is practically synchronous with the buildup of the photoproducts at 225 and 304 nm. The complete transformation of CBZ within just 60 min indicates the remarkable role of bromide salt in making the CBZ phototransformation much more efficient. In the absence of TiO_2, no significant degradation of CBZ was detected up to 5 h of irradiation, clearly indicating the possibility of a synergic effect between TiO_2 and NaBr in promoting the degradation reaction. No degradation activity was noted in the presence of catalyst under dark condition, this proved the photocatalytic nature of the reaction.

The influence of the initial NaBr concentration on CBZ photocatalyzed degradation was also investigated. The spectra recorded in the presence of 1.0×10^{-3}, 5.0×10^{-3} M and 5.0×10^{-2} M NaBr clearly showed similar shape over irradiation time (Fig. S4-S6), but a remarkable difference in the kinetic evolution of the degradation process emerged. To evaluate the effect of NaBr concentration on the reactivity of CBZ, observed rate constants (k_{obs}) were calculated by regression, using pseudo first-order rate relation Eq. (1), of concentration (C) data determined as absorbance at 280 nm at different irradiation times (see insets of Fig. 4 and Fig. S4-S6). Equation (1), obtained from the Langmuir–Hinshelwood model, is valid at low substrate concentration, so that there is no catalyst saturation and the intermediate adsorption can be neglected (Chiu et al., 2019). In this condition, k_{obs} depends on K, the reactant adsorption constant, and k_r, the effective reaction rate constant. Plotting k_{obs} values as a function of [NaBr] (Fig. 5), a deviation from linearity was observed with increasing concentration, likely because the salt may compete more and more with the pesticide for oxidizing sites on the TiO_2 surface (Wang and Wang, 2021; Abdullah et al., 1990).

$$C = C_0 e^{-k_r K t} = C_0 e^{-k_{obs} t} \quad (1)$$

To evaluate if the observed catalytic synergic effect of NaBr was peculiar of bromide, NaCl and NaI were tested both at a concentration of 1.0×10^{-2} M. As shown in Fig. S7, chloride clearly involved a slight effect on the photocatalytic efficiency of CBZ photodegradation within the same time in which the

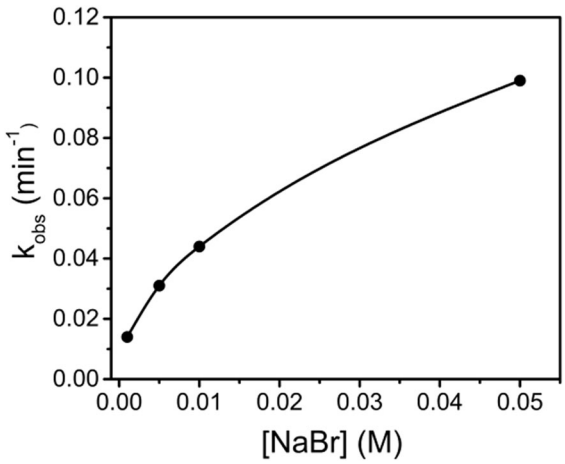

Fig. 5 Variation of observed rate constants (k_{obs}) of the photodegradation of 5.0×10^{-5} M CBZ (2.5×10^{-5} M after dilution with ethanol) catalyzed by 0.8 g/L TiO_2 in aqueous dispersion as a function of NaBr concentration

substrate completely disappeared in the presence of bromide. Iodide ions instead underwent oxidation in the reaction medium forming triiodide ions (Fig. S8), a hypothesis supported by the presence of bands centered at 288 and 360 nm which increased over time (Kireev and Shnyrev, 2015). The catalytic synergic action of Br^- ions in the CBZ photodegradation process was also tested using non-amphiphilic and amphiphilic quaternary ammonium salts, such as tetrabutylammonium bromide (TBABr) and cetyltrimethylammonium bromide (CTABr). As reported in Fig. S9 and S10, the shape of the absorption spectra, recorded over time in the presence of 1.0×10^{-2} M ammonium salts, were really identical to those obtained with NaBr. Differences instead were observed from the kinetic point of view; in fact, the pseudo-first order rate constants for the CBZ degradation, determined by Eq. (1) fitting (insets in Fig. S9 and S10) are lower than those obtained with NaBr ($k_{obs}=3.2\times10^{-2}$ and 1.8×10^{-2} min^{-1}, with TBABr and CTABr respectively, against 4.4×10^{-2} min^{-1} with NaBr). This data could be justified on the basis of the greater association of Br^- with the ammonium ion, as it is a cation softer than Na^+, resulting therefore less available to exert its catalytic action, especially when involved in CTABr micellar aggregates.

The CBZ photodegradation process by TiO_2 catalyst worked very well using sunlight in the presence of NaBr, as can be seen comparing the absorption spectra recorded with catalyst alone and together with 1.0×10^{-2} M NaBr (Fig. S11a and b, respectively). The pseudo-first order rate constant determined by data fitting of inset in Fig. S11b (1.7×10^{-2} min^{-1}) was 2.5 times lower than that obtained by UV lamp irradiation at 355 nm (4.4×10^{-2} min^{-1}), but a real parallel of the process efficiency was not possible as quantum yield data are not known. Anyway, this result indicates that utilization of sunlight can be a convenient source to drive such degradation reactions both from an economic and ecological point of view. The lack of photodegradation (Fig. S12) when LED lamps, (emitting exclusively visible light, Fig. S1) were used, suggests that only to the solar radiation at energy higher than ca. 400 nm is able of photolysis.

3.3 Analysis and Identification of Photodegradation Products of CBZ

HPLC–MS analyses to identify the photoproducts were carried out starting from more concentrated dispersions in CBZ and NaBr (2.0×10^{-4} M and 4.0×10^{-2} M, respectively) to satisfy the instrumental sensibility, as described in Experimental section. The spectral evolution recorded during photolysis is shown in Fig. S13. Analyses of irradiated samples allowed the identification of three main products, whose characteristics are collected in Table 1. In our HPLC-conditions, CBZ appeared at a retention time (RT) 4.11 min, with a protonated molecular ion peak ($M+H^+$) at m/z = 192.0776. Its assignment is endorsed by the comparison of the absorption spectrum recorded by HPLC–MS instrumentation (Fig. S14) with that of the pure sample (Fig. 1). The chromatographic peak area of CBZ, that decreased almost to zero within 610 min, was partially replaced by that of the P1 product peak with RT = 0.87 min and ($M+H^+$) at m/z = 118.0620. In turn, P1 area increased up to 190 min of irradiation and then decreased up to a tenth of its maximum value after 610 min (Fig. 6 and Table S1).

The shorter retention time is compatible with weaker interaction of P1 with the non polar stationary phase of C18 column, indicating the higher polarity of this product compared to CBZ. Moreover, the P1 absorption spectrum showed an increase in absorbance starting from 250 nm towards lower wavelengths (Fig S14), with maximum below 220 nm (in addition to an unidentified weak band centered at ca. 300 nm),

Table 1 CBZ and its degradation products with the corresponding molecular peaks and formula $(M+H)^+$, retention times (RT) and UV absorptions[a]

Compound	m/z $[M+H]^+$	Molecular formula	RT (min)	UV absorption λ (nm)
CBZ	192.0776	$C_9H_{10}N_3O_2$	4.11	245, 285
P1	118.0620	$C_3H_7N_3O_2$	0.87	208
P2	208.0725	$C_9H_{10}N_3O_3$	5.80	242, 285, 344 (sh)
P3	381.1314	$C_{18}H_{16}N_6O_4$	6.61	268 (sh), 300, 345(sh)

[a]Detected by HPLC–MS analysis during photodegradation of 2.0×10^{-4} M CBZ catalyzed by 0.8 g/L TiO_2 in aqueous dispersion in the presence of 4.0×10^{-2} M NaBr; sh stands for shoulder

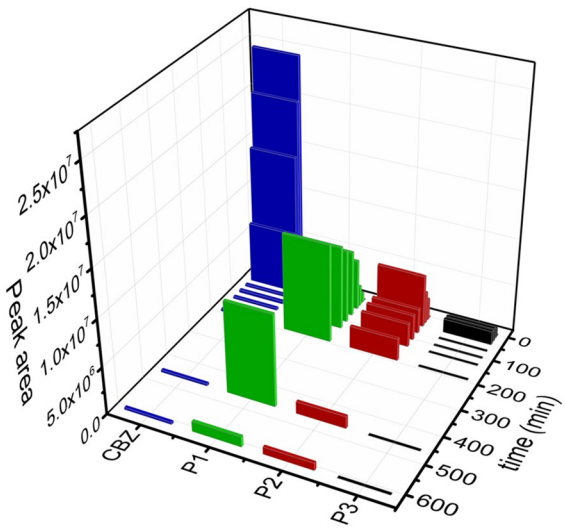

Fig. 6 Peak area evolution of CBZ and the photoproducts P1, P2 and P3 during the photodegradation of 2.0×10^{-4} M CBZ (1.0×10^{-4} M after dilution with acetonitrile) catalyzed by 0.8 g/L TiO_2 in aqueous dispersion in the presence of 4.0×10^{-2} M NaBr. Peak area values of CBZ are divided by 5

in agreement with a poorly conjugated structure. Based on this evidence, P1 was identified as 1-(methoxycarbonyl)guanidine (Fig. 7), which is a product already detected in CBZ samples coming from UV direct photolysis (Boudina et al., 2003; Mazellier et al., 2002), TiO_2 heterogeneous photocatalysis (Calza et al., 2006) and homogeneous photooxidation (Da Costa et al., 2019). Abdou et al. (1985) proposed the formation of 1-(methoxycarbonyl)guanidine by direct photolysis of CBZ with a mechanism that implied radical or bi-radical species produced from cleavage of the benzimidazole ring, generating a benzene or dihydroxybenzene. It is surprising that in our experimental conditions, in which a radiation poorly absorbed by CBZ was used, such a product can be observed. On the other hand, large amount of this product was found in the CBZ degradation photocatalyzed by TiO_2 under xenon lamp radiation equipped with a 340 nm cutoff filter (Calza et al., 2006). In this work, an association of the pesticide to the TiO_2 surface, by interaction of the CBZ basic nitrogen and oxygen atoms with surface-bound Ti(IV) ions, was hypothesized, which caused a spectral red shift. This effect was also invoked for TiO_2 photocatalysis of fluoroquinolones (Paul et al., 2007).

After $R_t = 5.80$ min, the mass spectrum showed a protonated molecular ion peak at m/z = 208.0725, which was assigned to hydroxycarbendazim structure P2 shown in Fig. 7. Such assignment is supported by Temgoua et al. (2021), who detected a compound with the same mass in the CBZ oxidative degradation,

Fig. 7 Structures of the degradation products

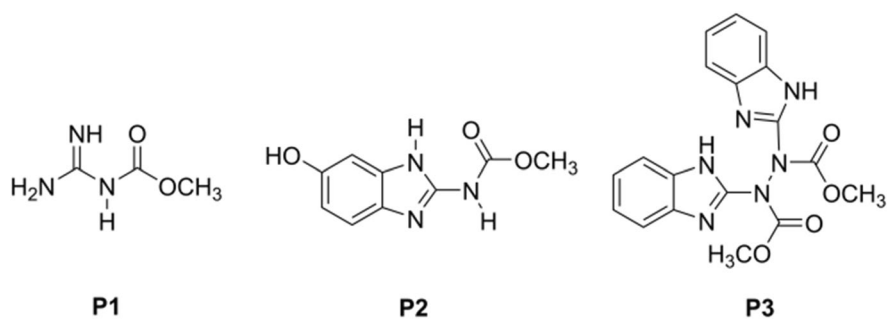

carried out by electrochemistry coupled to high resolution mass spectrometry, which was identified as structure P2. As reported by the authors, DFT calculations endorsed the hydroxylation at the aromatic carbon atom in meta position respect to imidazole NH, this being more electrophilic center and allowing to restore aromaticity more easily. As observed in Fig. 6, the P2 formation was parallel to that of P1, reaching maximum concentration within 40 min of irradiation consequently to the CBZ disappearance. Finally, at a higher retention time (6.61 min), HPLC–MS analysis allowed to identify more isomers corresponding to *m/z* 381.1314, attributed to dimers produced by coupling of reactive intermediates formed during CBZ oxidation. Still in agreement with Temgoua et al. (2021), we propose the structure P3 of Fig. 7 as the most prevailing for the CBZ-CBZ dimer, indicated by the authors as the most plausible on the base of the maximum spin-density, determined by density functional theory (DFT) calculation, on the deprotonated nitrogen atom. The P3 concentration increased at shorter irradiation times (until 40 min, Table S1), when a substantial amount of CBZ was still available, after that no detectable trace was observed. As for the UV absorption spectra, both P2 and P3 showed a red shift with respect to CBZ (Fig S14). In particular, P2 showed two broad bands centered at 247 and 290 nm, with the second extending to 325 nm, while with P3 the maxima shifted to 252 and 313 nm. By comparing these spectra with those recorded during CBZ photolysis at different irradiation times (Fig. S13), we can assign the band around 300 nm, which becomes more and more intense and shifts towards longer wavelengths with the time irradiation, to the formation of P2 and P3. Indeed, the pseudo-first order fitting of the CBZ decay at 280 nm produced a rate constant of 2.1×10^{-2} min^{-1}, a value close to that calculated by a first order grow-decay fitting at 304 nm equal to1.6×10^{-2} min^{-1} (Fig. S13 inset). This result suggests that, despite the inevitable spectral overlap, at 280 nm CBZ mainly absorbs, while at 304 nm the P2 absorbance is prevalent, taking into account that from the HPLC–MS analysis P3 resulted in small quantities and present only at shorter irradiation times. A similar temporal spectral evolution was also observed for the experiments carried out at lower CBZ concentration (5.0×10^{-5} M, Fig. 4, S6, S9 and S10). In particular, in the experiment carried out in the presence of 5.0×10^{-2} M NaBr (Fig. S6), the CBZ decay at 280 nm ($k_{obs}=1.0\times10^{-1}$ min^{-1} determined by mono-exponential fitting) was perfectly coupled with the absorbance at 304 nm ($k_{obs}=1.1\times10^{-1}$ min^{-1}, determined by bi-exponential fitting), wavelength at which only P2 should absorb, as the formation of dimer P3 should not be favored due to more diluted dispersion of CBZ.

Some authors detected, after direct photolysis, others by-products, such as 2-aminobenzimidazole and benzimidazole isocyanate, known to be generated from the CBZ excited state (Boudina et al., 2003; Calza et al., 2006). Identical species were observed in CBZ removal by solar photo-Fenton (Da Costa et al., 2019). In this work the formation of these products was assumed due to the intervention of powerful oxidant $OH^{\bullet}$, which is considered the main responsible for the degradation of various pollutants in TiO_2-mediated heterogeneous photocatalysis (da Silva et al., 2023; Jiang et al., 2021). In our experiments, 2-aminobenzimidazole and benzimidazole isocyanate were not detected and this was convenient taking into account that they are even more toxic than CBZ (Jiang et al., 2021; Temgoua et al., 2021).

3.4 Proposed Mechanism for the Bromide-assisted TiO_2-photocatalyzed Degradation of CBZ

The experimental results were rationalized according to the mechanism depicted in Fig. 8. As already stated, from comparison with literature data, the P1 formation path should involve radical and/or diradical species produced by photoexcitation of TiO_2 surface-associated CBZ molecules (Abdou et al., 1985; Paul et al., 2007).

Since products P2 and P3 match with those detected in electrochemically degraded CBZ solution (Temgoua et al., 2021), similarly we propose that also the TiO_2 photocatalyzed degradation of CBZ could start by a single electron transfer (SET) from CBZ to the hole photogenerated in the valence band, producing radical cation $CBZ^{\bullet+}$. This is supported by the negative free energy change ($\Delta G_{ET}=-1.1$ eV) calculated from the reduction potential of valence band h^{+}_{VB} (2.50 V vs SCE; Zhonga et al., 2019) and the CBZ oxidation potential (1.4 V vs SCE; Manisankar et al., 2006). On the other hand, the one-electron oxidation potential of H_2O is estimate to be 2.07 V vs. SCE at pH 7 (Armstrong et al., 2013), therefore it is thermodynamically possible that H_2O can also

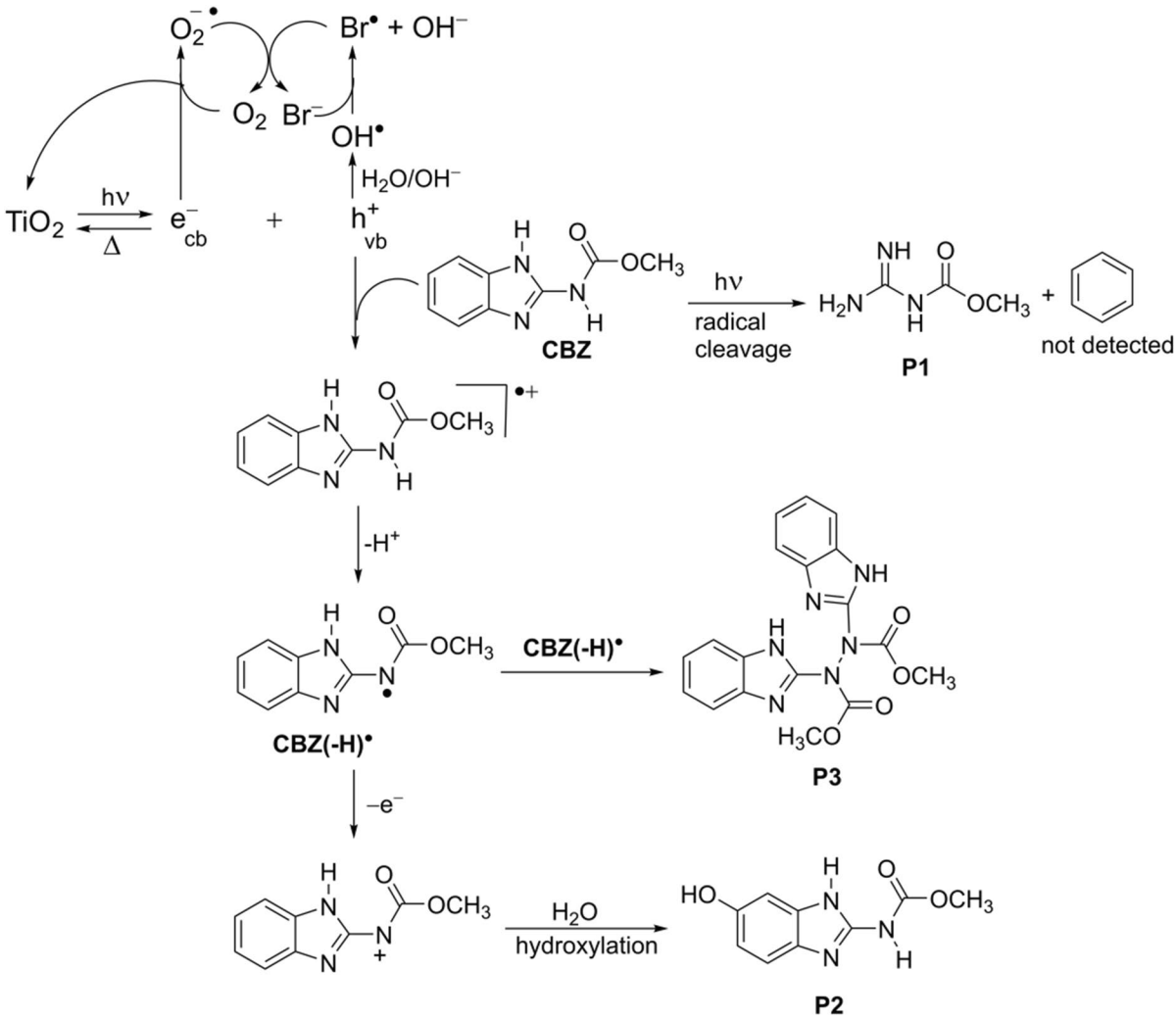

Fig. 8 Schematic diagram of reaction intermediate formation during CBZ photocatalytic degradation

react competitively with h_{VB}^{+} to form radicals $OH^{\bullet}$ ($\Delta G_{ET} = -0.43$ eV).

Due to the more negative value of ΔG_{ET}, CBZ direct oxidation by the hole should be favored, despite that the water molecules present in great excess and constituting the first adsorption (Parrino et al., 2020). On the other hand, CBZ adsorption could improve thanks to an electrostatic pushing effect of bromide ions (salting-out effect) due to an increase in ionic strength that would cause a decrease in solubility of the neutral pesticide (Sarkar et al., 2010). In addition, since the point of zero charge (pzc) of TiO_2 P25 spans between 5.4 to 6.3 (Bourikas et al., 2003; Zhu et al., 2005), at distilled water pH employed (5.5 – 6.0) both semiconductor surface and CBZ should be in neutral form. Therefore, very efficient hydrogen- bonding interactions is established between carbonyl oxygen, imidazolic nitrogen and amide nitrogen with the surface hydroxyl groups bonded to titanium. The strong interaction between CBZ and TiO_2 is in agreement with a direct oxidation, as already suggested by Villarreal et al. (2004). As a matter of fact, according to the authors, the oxidation of organics with strong interaction on TiO_2 nanoparticles proceeded via direct hole transfer pathway, as opposed to the weak-interacting substrates, for which indirect mechanism by $OH^{\bullet}$ radicals dominated the oxidation reaction.

Once radical cation $CBZ^{\bullet+}$ is generated, it undergoes deprotonation at the amidic nitrogen forming radical $CBZ(-H)^{\bullet}$. This radical is particularly predisposed to be involved in dimer formation according to structure P3. The formation of dimeric structures is peculiar of high concentration and therefore not of interest for environmental degradation. Anyway, the dimer detection is useful from a mechanistic point of view, as it depends on the presence of radicals, and this endorses a SET reaction as primary step. A SET mechanism was already proposed for the formation of dimers in the CBZ degradation photosensitized by aromatic ketones, supported by flash photolysis detection of the key transients (Jornet et al., 2013). Even in TiO_2-mediated photochemical oxidation occurring by SET mechanism, dimer formation is already known. For example, substituted benzyltrimethylsilanes produced diarylethanes with good yields, thanks to the presence of a relatively high concentration of benzyl radicals adsorbed onto the semiconductor surface (Baciocchi et al., 1992). The $CBZ(-H)^{\bullet}$ reaction to form dimers is assumed to be in competition with that of oxidation by a second positive hole to produce carbocation $CBZ(-H)^{+}$, which in turn undergoes, by H_2O attack, a hydroxylation reaction to yield P2. Free $OH^{\bullet}$ radicals are known not to react by one-electron transfer (Minero et al., 2000), but the hydroxyl radical attack to the CBZ aromatic rings cannot be entirely excluded (Liu et al., 2022), although this attack generally leads to a low selectivity, contrary to what happens when the hydroxylation product is generated by a SET mechanism (Temgoua et al., 2021).

Oxygen generally improves the photocatalytic degradation of organic contaminants because it prevents the recombination of electron–hole pairs by electron trapping yielding superoxide anion $O_2^{\bullet-}$ (as shown in Fig. 8). This reaction is thermodynamically favored, as evidenced by the redox potentials, that are $E^0_{TiO2/(TiO2)e-} = -0.76$ V (Fujishima et al., 2000) and $E^0_{O2/O2^{\bullet-}} = -0.42$ V (Armstrong et al., 2013), both vs. SCE. The low degradation efficiency detected for the air-equilibrated CBZ reaction in the presence of only TiO_2 (Fig. 3) clearly indicates that both oxygen reduction and pesticide oxidation reactions are not significantly competitive with that of electron–hole recombination. As shown, addition of bromide salt was found to improve strikingly the catalytic efficiency of the CBZ photoreaction and this effect is tentatively explained as follows. Radicals $Br^{\bullet}$, generated by Br^{-}one-electron oxidation with $OH^{\bullet}$ ($E^0_{Br\bullet/Br-} = 1.72$ V against $E^0_{OH\bullet/H2O} = 2.07$ V vs. SCE; Armstrong et al., 2013), are in turn reduced back to bromide ions by $O_2^{\bullet-}$ ($E^0_{O2/O2^{\bullet-}} = -0.42$ V vs. SCE; Armstrong et al., 2013) as schematically shown in Fig. 8. This reaction promotes the electron capture in the conduction band by oxygen, preventing the $O_2^{\bullet-}$ back electron transfer reaction, as well as it increases the oxygen concentration near the semiconductor surface. In line with this pattern, the reduced effect of NaCl on the photocatalytic degradation efficiency of CBZ is explainable taking into account that chloride ions are more difficult to oxidize by hydroxide radicals ($E^0_{Cl\bullet/Cl-} = 2.19$ V against $E^0_{OH\bullet/H2O} = 2.07$ V vs. SCE; Armstrong et al., 2013). The promotion of the CBZ photocatalytic degradation by halide addition was unexpected as it was observed only in very few cases (Abdullah et al., 1990; Minero et al., 2000). Generally, inorganic ions, in particular halides, were found, even very recently, to inhibit photocatalytic oxidation of organic pollutants, specially by $OH^{\bullet}$ scavenging effect and adsorption competition on the catalyst surface (Abdullah et al., 1990; Calza and Pelizzetti, 2001; Dugandžic et al., 2017; Guillard et al., 2005;).

The formation of radicals $Br^{\bullet}$ is supported by very small traces of mono-brominated products detected by HPLC–MS analysis (Fig. S15), including one having formula $C_9H_8BrN_3O_2$ (m/z = 269.9873), which was assigned to the product formed by association of radicals $CBZ(-H)^{\bullet}$ with $Br^{\bullet}$. The eventuality that bromine atom can react with a bromide ion forming radical anion $Br_2^{\bullet-}$, intermediate leading to molecular bromine production, is ruled out from the lack of the characteristic bromine absorption band at 415 nm in the recorded spectra (Parrino et al., 2020). The action of Br^{-} as $OH^{\bullet}$ scavenger would also explain the absence of benzimidazole isocyanate and 2-aminobenzimidazole in the reaction mixture, whose formation was suggested to be due to the intervention of hydroxyl radicals (Da Costa et al., 2019). The catalysis increase observed by increasing bromide concentration (Fig. 5), despite the Br^{-} action as $OH^{\bullet}$ scavenger, leads to excluding a direct involvement of hydroxyl radicals in the oxidation reaction of the pesticide. Therefore, the oxidation by the holes should be the dominant pathway of starting the CBZ degradation process.

The involvement of $OH^{\bullet}$ and O_2 in the semiconductor regeneration process was supported by experiments performed in the presence of CH_3OH, an efficient $OH^{\bullet}$ scavenger (Schneider et al., 2020), and by bubbling argon to remove oxygen from the suspension (Fig. S16 and S17, respectively).In both cases, in accordance with the proposed mechanism, a dramatic reduction of the photocatalytic degradation efficiency was detected.

4 Conclusions

In the present work, the CBZ removal from water activated by TiO_2 photocatalysis under near-UV light irradiation in air-equilibrated condition and in the presence of bromide salts was successfully achieved. Special attention was paid to the identification and kinetics of the intermediates involved in the process, in order to elucidate the photodegradation mechanism. In particular, the observed intermediate distribution was discussed according to a degradation process initiated by a direct hole oxidation pathway rather than by a $OH^{\bullet}$ attacking mechanism. The role played by radicals $OH^{\bullet}$ instead was that to oxidize bromide to bromine atoms, which regenerate oxygen by superoxide radical oxidation. This effect may be associated with a better separation between photogenerated holes and electrons.

Finally, it is interesting, from an ecological point of view, that photodegradation by TiO_2 photocatalysis, potentiated by addition of non-toxic salt and using outside solar light as a source of irradiation, led to the almost complete disappearance of CBZ in a short time. Accordingly, this methodology could provide a promising way for achieving an efficient and more sustainable photocatalytic oxidation.

Acknowledgements We acknowledge University of Perugia and MUR for support within the project Vitality.

Funding Open access funding provided by Università degli Studi di Perugia within the CRUI-CARE Agreement. This work has been funded by the European Union—NextGenerationEU under the Italian Ministry of University and Research (MUR) National Innovation Ecosystem grant ECS00000041—VITALITY.

Data Availability The authors state that all data analyzed during this study are included in the article and supplementary materials.

Declarations

Conflict of Interest There are no conflicts to declare.

References

Abdou, W. M., Mahran, M. R., Sidky, M. M., & Wamhoff, H. (1985). Photochemistry of pesticides, 3: Photolysis of methyl 2-benzimidazolecarbamate (Carbendazim) in the presence of singlet oxygen. *Chemosphere, 14*(9), 1343–1353. https://doi.org/10.1016/0045-6535(85)90155-9

Abdullah, M., Low, G. K.-C., & Matth, R. W. (1990). Effects of common inorganic anions on rates of photocatalytic oxidation of organic carbon over illuminated titanium dioxide. *Journal of Physical Chemistry*, *94*, 6820–6825. 0022–3654/90/2094–6820S02.50/0

Ádám, B., Cocco, P., & Godderis, L. (2024). Hazardous effects of pesticides on human health. *Toxics, 12*(3), 186. https://doi.org/10.3390/toxics12030186

Anastasio, P., Del Giacco, T., Germani, R., Spreti, N., & Tiecco, M. (2017). Structure effects of amphiphilic and non-amphiphilic quaternary ammonium salts on photodegradation of Alizarin Red-S catalyzed by titanium dioxide. *RSC Advances, 7*, 361–368. https://doi.org/10.1039/C6RA25421G

Armstrong, D. A., Huie, R. E., Lymar, S., Koppenol, W. H., Merényi, G., Neta, P., Stanbury, D. M., Steenken, S., & Wardman, P. (2013). Standard electrode potentials involving radicals in aqueous solution: Inorganic radicals. *BioInorganic Reaction Mechanisms, 9*(1–4), 59–61. https://doi.org/10.1515/irm-2013-0005

Baciocchi, E., Rol, C., Rosato, G. C., & Sebastiani, G. V. (1992). Titanium dioxide photocatalysed oxidation of benzyltrimethylsilanes in the presence of silver sulfate. *Journal of the Chemical Society, Chemical Communications, 1*, 59–41. https://doi.org/10.1039/C39920000059

Baglioni, P., Braccalenti, E., Carretti, E., Germani, R., Goracci, L., Savelli, G., & Tiecco, M. (2009). Surfactant-based photorheological fluids: Effect of the surfactant structure. *Langmuir, 25*(10), 5467–5475. https://doi.org/10.1021/la900465h

Boudina, A., Emmelin, C., Baaliouamer, A., Grenier-Loustalot, M. F., & Chovelon, J. M. (2003). Photochemical behaviour of carbendazim in aqueous solution. *Chemosphere, 50*(5), 649–655. https://doi.org/10.1016/S0045-6535(02)00620-3

Bourikas, K., Vakros, J., Kordulis, C., & Lycourghiotis, A. (2003). Potentiometric mass titrations: Experimental and theoretical establishment of a new technique for determining the point of zero charge (PZC) of metal (hydr)oxides. *Journal of Physical Chemistry B, 107*, 9441–9451. https://doi.org/10.1080/03067310500247959

Calza, P., & Pelizzetti, E. (2001). Photocatalytic transformation of organic compounds in the presence of inorganic ions. *Pure and Applied Chemistry, 73*(12), 1839–1848. https://doi.org/10.1351/pac200173121839

Calza, P., Medana, C., Baiocchi, C., & Pelizzetti, E. (2006). Light-induced transformations of fungicides on titanium dioxide: Pathways and by-products evaluation using the LC-MS technique. *International Journal of Environmental Analytical Chemistry, 86*, 265–275. https://doi.org/10.1080/03067310500247959

Cheng, Y., & Li, H. (2022). Efficient degradation of Carbendazim by ferrate(VI) oxidation under near-neutral conditions. *Sustainability, 14*(20), 13678. https://doi.org/10.3390/su142013678

Cheng, M., Zeng, G., Huang, D., Lai, C., Xu, P., Zhang, C., & Liu, Y. (2016). Hydroxyl radicals based advanced oxidation processes (AOPs) for remediation of soils contaminated with organic compounds: A review. *Chemical Engineering Journal, 284*, 582–598. https://doi.org/10.1016/j.cej.2015.09.001

Chiu, Y.-H., Chang, T.-F.M., Chen, C.-Y., Sone, M., & Hsu, Y.-J. (2019). Mechanistic insights into photodegradation of organic dyes using heterostructure photocatalysts. *Catalysts, 9*(5), 430. https://doi.org/10.3390/catal9050430

Da Costa, E. P., Bottrel, S. E. C., Starling, M., Leao, M. M. D., & Amorim, C. C. (2019). Degradation of carbendazim in water via photo-Fenton in raceway pond reactor: Assessment of acute toxicity and transformation products. *Environmental Science and Pollution Research, 26*, 4324–4336. https://doi.org/10.1007/s11356-018-2130-z

da Silva, J. R. Q., Almeida, P. F., Santos, L. E. R., & Brugnera, M. F. (2023). TiO_2 nanotubes impregnated with Au nanoparticles: Characterization and application in carbendazim and atrazine degradation. *Journal of Photochemistry and Photobiology, A: Chemistry, 438*, 114567. https://doi.org/10.1016/j.jphotochem.2023.114567

Del Giacco, T., Germani, R., Saracino, F., & Stradiotto, M. (2017). Counterion effect of cationic surfactants on the oxidative degradation of Alizarin Red-S photocatalysed by TiO_2 in aqueous dispersion. *Journal of Photochemistry and Photobiology A: Chemistry, 332*, 546–553. https://doi.org/10.1016/j.jphotochem.2016.10.002

Dos Santos, E. V., Sáez, C., Cañizares, P., Martínez-Huitle, C. A., & Rodrigo, M. A. (2017). UV assisted electrochemical technologies for the removal of oxyfluorfen from soil washing wastes. *Chemical Engineering Journal, 318*, 2–9. https://doi.org/10.1016/j.cej.2016.03.015

Dugandžic, A. M., Tomaševic, A. V., Radišic, M. M., Šekuljica, N. Ž, Mijinc, D. Ž, & Petrovic, S. D. (2017). Effect of inorganic ions, photosensitisers and scavengers on the photocatalytic degradation of nicosulfuron. *Journal of Photochemistry and Photobiology A: Chemistry, 336*, 146–155. https://doi.org/10.1016/j.jphotochem.2016.12.031

Fujishima, A., Rao, T. N., & Tryk, D. A. (2000). Titanium dioxide photocatalysis. *Journal of Photochemistry and Photobiology C: Photochemistry Reviews, 1*(1), 1–21. https://doi.org/10.1016/S1389-5567(00)00002-2

Furini, L. N., Constantino, C. J. L., Sanchez-Cortes, S., Otero, J. C., & López-Tocón, I. (2016). Adsorption of carbendazim pesticide on plasmonic nanoparticles studied by surface-enhanced Raman scattering. *Journal of Colloid and Interface Science, 465*, 183–189. https://doi.org/10.1016/j.jcis.2015.11.045

Germani, R., Bini, M., Fantacci, S., Simonetti, F., Tiecco, M., Vaioli, E., & Del Giacco, T. (2021). Influence of surfactants in improving degradation of polluting dyes photocatalyzed by TiO_2 in aqueous dispersion. *Journal of Photochemistry and Photobiology A: Chemistry, 418*, 113342. https://doi.org/10.1016/j.jphotochem.2021.113342

Germani, R., Mancinelli, M., Roselli, A., Tiecco, M., Fantacci, S., Di Bona, S., & Del Giacco, T. (2023). Kinetic effects of cationic surfactants on the photocatalytic degradation of anionic dyes in aqueous TiO_2 dispersions. *New Journal of Chemistry, 47*, 392–401. https://doi.org/10.1039/D2NJ04715B

Ghamarpoor, R., Fallah, A., & Jamshidi, M. (2024). A Review of synthesis methods, modifications, and mechanisms of ZnO/TiO_2-based photocatalysts for photodegradation of contaminants. *ACS Omega, 9*, 25457–25492. https://doi.org/10.1021/acsomega.3c08717

Guillard, C., Puzenat, E., Lachheb, H., Houas, A., & Herrmann, J.-M. (2005). Why inorganic salts decrease the TiO_2 photocatalytic efficiency. *International Journal of Photoenergy, 7*, 1–9. https://doi.org/10.1155/S1110662X05000012

Hadei, M., Mesdaghinia, A., Nabizadeh, R., Mahvi, A. H., Rabbani, S., & Naddafi, K. (2021). A comprehensive systematic review of photocatalytic degradation of pesticides using nano TiO_2. *Environmental Science and Pollution Research, 28*, 13055–13071. https://doi.org/10.1007/s11356-021-12576-8

Hu, Y., & Liu, Y. (2024). Impact of fertilizer and pesticide reductions on land use in China based on crop-land integrated model. *Land Use Policy, 141*, 107155. https://doi.org/10.1016/j.landusepol.2024.107155

Jiang, D., Otitoju, T. A., Ouyang, Y., Shoparwe, N. F., Wang, S., Zhang, A., & Li, S. (2021). A Review on metal ions modified TiO_2 for photocatalytic degradation of organic pollutants. *Catalysts, 11*(9), 1039. https://doi.org/10.3390/catal11091039

Jornet, D., Castillo, M. A., Sabater, M. C., Tormos, R., & Miranda, M. A. (2013). Photodegradation of carbendazim sensitized by aromatic ketones. *Journal of Photochemistry and Photobiology A: Chemistry, 256*, 36–41. https://doi.org/10.1016/j.jphotochem.2013.02.004

Kanan, S., Moyet, M. A., Arthur, R. B., & Patterson, H. H. (2020). Recent advances on TiO_2-based photocatalysts toward the degradation of pesticides and major organic pollutants from water bodies. *Catalysis Reviews, 62*(1), 1–65. https://doi.org/10.1080/01614940.2019.1613323

Kaur, T., Sraw, A., Wanchoo, R. K., & Toor, A. P. (2016). Visible –light induced photocatalytic degradation of fungicide with Fe and Si doped TiO_2 nanoparticles. *Materials Today: Proceedings, 3*(2), 354–361. https://doi.org/10.1016/j.matpr.2016.01.020

Kaur, R., Choudhary, D., Bali, S., Bandral, S. S., Singh, V., Ahmad, M. A., Rani, N., Singh, T. G., & Chandrasekaran, B. (2024). Pesticides: An alarming detrimental to health and environment. *Science of the Total Environment, 915*, 170113. https://doi.org/10.1016/j.scitotenv.2024.170113

Khan, N. A., Khan, S. U., Ahmed, S., Farooqi, I. H., Yousefi, M., Mohammadi, A. A., & Changani, F. (2020). Recent trends in disposal and treatment technologies of emerging-pollutants-a critical review. *Trends in Analytical Chemistry, 122*, 115744. https://doi.org/10.1016/j.trac.2019.115744

Khmelevtsova, L., Azhogina, T., Karchava, S., Klimova, M., Polienko, E., Litsevich, A., Chernyshenko, E., Khammami, M., Sazykin, I., & Sazykina, M. (2024). Effect of Mineral Fertilizers and Pesticides Application on Bacterial Community and Antibiotic-Resistance Genes Distribution in Agricultural Soils. *Agronomy, 14*(5), 1021. https://doi.org/10.3390/agronomy14051021

Kireev, S. V., & Shnyrev, S. L. (2015). Study of molecular iodine, iodate ions, iodide ions, and triiodide ions solutions absorption in the UV and visible light spectral bands. *Laser Physics, 25*, 075602. https://doi.org/10.1088/1054-660X/25/7/075602

Liu, W., Li, Y., Wang, Y., Zhao, Y., Xu, Y., & Liu, X. (2022). DFT insights into the degradation mechanism of carbendazim by hydroxyl radicals in aqueous solution. *Journal of Hazardous Materials, 431*, 128577. https://doi.org/10.1016/j.jhazmat.2022.128577

Machado, R. M., da Silva, S. W., Bernardes, A. M., & Ferreira, J. Z. (2022). Degradation of carbendazim in aqueous solution by different settings of photochemical and electrochemical oxidation processes. *Journal of Environmental Management, 310*, 114805. https://doi.org/10.1016/j.jenvman.2022.114805

Manisankar, P., Selvanathan, G., & Vedhi, C. (2006). Determination of pesticides using heteropolyacid montmorillonite clay-modified electrode with surfactant. *Talanta, 68*(3), 686–692. https://doi.org/10.1016/j.talanta.2005.05.021

Marcelino, R. B. P., Amorim, C. C., Ratova, M., Delfour-Peyrethonb, B., & Kelly, P. (2019). Novel and versatile TiO_2 thin films on PET for photocatalytic removal of contaminants of emerging concern from water. *Chemical Engineering Journal, 370*, 1251–1261. https://doi.org/10.1016/j.cej.2019.03.284

Mazellier, P., Leroy, É., & Legube, B. (2002). Photochemical behavior of the fungicide carbendazim in dilute aqueous solution. *Journal of Photochemistry and Photobiology A: Chemistry, 153*, 221–227. https://doi.org/10.1016/S1010-6030(02)00296-4

Minero, C., Mariella, G., Maurino, V., & Pelizzetti, E. (2000). Photocatalytic transformation of organic compounds in the presence of inorganic anions. 1. Hydroxyl-mediated and direct electron-transfer reactions of phenol on a titanium dioxide-fluoride system. *Langmuir, 16*, 2632–2641. https://doi.org/10.1021/la9903301

Murgolo, S., De Ceglie, C., Di Iaconi, C., & Mascolo, G. (2021). Novel TiO_2-based catalysts employed in photocatalysis and photoelectrocatalysis for effective degradation of pharmaceuticals (PhACs) in water: A short review. *Current Opinion in Green and Sustainable Chemistry, 30*, 100473. https://doi.org/10.1016/j.cogsc.2021.100473

Parrino, F., Livraghi, S., Giamello, E., Ceccato, R., & Palmisano, L. (2020). Role of hydroxyl, superoxide, and nitrate radicals on the fate of bromide ions in photocatalytic TiO_2 suspensions. *ACS Catalysis, 10*, 7922–7931. https://doi.org/10.1021/acscatal.0c02010

Paul, T., Miller, P. L., & Strathmann, T. J. (2007). Visible-light-mediated TiO_2 photocatalysis of fluoroquinolone antibacterial agents. *Environmental Science & Technology, 41*, 4720–4727. https://doi.org/10.1021/es070097q

Rengifo-Herrera, J. A., & Pulgarin, C. (2023). Why five decades of massive research on heterogeneous photocatalysis, especially on TiO_2, has not yet driven to water disinfection and detoxification applications? Critical review of drawbacks and challenges. *Chemical Engineering Journal, 477*, 14687. https://doi.org/10.1016/j.cej.2023.146875

Rostami, M., Badiei, A., Ganjali, M. R., Rahimi-Nasrabadi, M., Naddafi, M., & Karimi-Maleh, H. (2022). Nano-architectural design of TiO_2 for high performance photocatalytic degradation of organic pollutant: A review. *Environmental Research, 212*(Part D), 113347. https://doi.org/10.1016/j.envres.2022.113347

Saleh, I. A., Zouari, N., & Al-Ghouti, M. A. (2020). Removal of pesticides from water and wastewater: Chemical, physical and biological treatment approaches. *Environmental Technology & Innovation, 19*, 101026. https://doi.org/10.1016/j.eti.2020.101026

Sarkar, D., Ghosh, D., Das, P., & Chattopadhyay, N. (2010). Electrostatic pushing effect: A prospective strategy for enhanced drug delivery. *Journal of Physical Chemistry, B, 114*, 12541–12548. https://doi.org/10.1021/jp1049099

Schneider, J. T., Firak, D. S., Ribeiro, R. R., & Peralta-Zamora, P. (2020). Use of scavenger agents in heterogeneous photocatalysis: Truths, half-truths, and misinterpretations. *Physical Chemistry Chemical Physics, 22*, 15723–15733. https://doi.org/10.1039/D0CP02411B

Shamim, A., Neelam, K., Kamaal, S., Ali, A., & Ahmad, M. (2024). Removal of pesticide pollutants from aqueous waste utilizing nanomaterials via photocatalytic process: A review. *International Journal of Environmental Science and Technology, 21*, 4653–4684. https://doi.org/10.1007/s13762-023-05341-6

Sousa, J. C. G., Ribeiro, A. R., Barbosa, M. O., Pereira, M. F. R., & Silva, A. M. T. (2018). A review on environmental monitoring of water organic pollutants identified by EU guidelines. *Journal of Hazardous Materials, 344*, 146–162. https://doi.org/10.1016/j.jhazmat.2017.09.058

Starling, M. C. V. M., Souza, P. P., Le Person, A., Amorim, C. C., & Criquet, J. (2019). Intensification of UV-C treatment to remove emerging contaminants by UVC/ H_2O_2 and UV-C/$S_2O_8^{2-}$: Susceptibility to photolysis and investigation of acute toxicity. *Chemical Engineering Journal, 376*, 120856. https://doi.org/10.1016/j.cej.2019.01.135

Tahmasebia, A. A., Tabatabaei, Z., Azhdarpoorb, A., & Benia, A. S. (2024). Evaluation of phosphate insecticides and common herbicides: Monitoring and risk assessment in

water treatment plant, distribution networks, and underground water wells. *Journal of Water and Health, 22*, 1089. https://doi.org/10.2166/wh.2024.076

Temgoua, R. C. T., Bussy, U., Alvarez-Dorta, D., Galland, N., Hèmez, J., Thobie-Gautier, C., Tonlé, I. K., & Boujtita, M. (2021). Using electrochemistry coupled to high resolution mass spectrometry for the simulation of the environmental degradation of the recalcitrant fungicide carbendazim. *Talanta, 221*, 121448. https://doi.org/10.1016/j.talanta.2020.121448

Varma, K. S., Tayade, R. J., Shah, K. J., Joshi, P. A., Shukla, A. D., & Gandhi, V. G. (2020). Photocatalytic degradation of pharmaceutical and pesticide compounds (PPCs) using doped TiO_2 nanomaterials: A review. *Water-Energy Nexus, 3*, 46–61. https://doi.org/10.1016/j.wen.2020.03.008

Villarreal, T. L., Gomez, R., Gonzalez, M., & Salvador, P. (2004). A kinetic model for distinguishing between direct and indirect interfacial hole transfer in the heterogeneous photooxidation of dissolved organics on TiO_2 nanoparticle suspensions. *Journal of Physical Chemistry B, 108*, 20278–20290. https://doi.org/10.1021/jp046539r

Wang, J., & Wang, S. (2021). Effect of inorganic anions on the performance of advanced oxidation processes for degradation of organic contaminants. *Chemical Engineering Journal, 411*, 128392. https://doi.org/10.1016/j.cej.2020.128392

Xiao, J., Xie, Y., & Cao, H. (2015). Organic pollutants removal in wastewater by heterogeneous photocatalytic ozonation. *Chemosphere, 121*, 1–17. https://doi.org/10.1016/j.chemosphere.2014.10.072

Yadav, I. C., & Devi, N. L. (2017). Pesticides classification and its impact on human and environment. In Kumar, A., Singhal, J. C., Techato, K., Molina, L. T., Singh, N., Kumar, P., Kumar, P., Chandra, R., Caprio, S., Upadhye, S., Yonemura, S., Rao, S. Y., Zhang, T. C., Sharma, U. C., & Abrol, Y. P. (Eds.), *Environmental Engineering Science* (Vol. 6: Toxicology, Chapter: 7, pp. 140–158). Studium Press LLC.

Zhonga, J., Zhao, Y., Ding, L., Ji, H., Ma, W., Chen, C., & Zhao, J. (2019). Opposite photocatalytic oxidation behaviors of BiOCl and TiO_2: Direct hole transfer vs. indirect $^{\bullet}OH$ oxidation. *Applied Catalysis B: Environmental, 241*, 514–520. https://doi.org/10.1016/j.apcatb.2018.09.058

Zhou, T., Guo, T., Wang, Y., Wang, A., & Zhang, M. (2023). Carbendazim: Ecological risks, toxicities, degradation pathways and potential risks to human health. *Chemosphere, 314*, 137723. https://doi.org/10.1016/j.chemosphere.2022.137723

Zhu, X., Yuan, C., Bao, Y., Yang, J., & Wu, Y. (2005). Photocatalytic degradation of pesticide pyridaben on TiO_2 particles. *Journal of Molecular Catalysis A: Chemical, 229*(1–2), 95–105. https://doi.org/10.1016/j.molcata.2004.11.010